Chemistry—Methods

Research Article
doi.org/10.1002/cmtd.202500090

Chemistry Europe
European Chemical Societies Publishing

www.chemistrymethods.org

Generation of Pseudo Metabolites as a Side Reaction in On-Tissue Chemical Derivatization in Matrix-Assisted Laser Desorption/Ionization Mass Spectrometry Imaging

Tobias Bausbacher, Alessa L. Henneberg, Stephanie Meyer, Stefan Schmidt, Aubry K. Miller, Christiane A. Opitz, and Carsten Hopf*

Matrix-assisted laser desorption/ionization mass spectrometry imaging (MALDI-MSI) is a key spatial omics technology for spatially resolved visualization and direct on-tissue identification of multiple lipid and metabolite classes. Recently, many on-tissue chemical derivatization (OTCD) reagents targeting defined functional groups have been introduced to improve sensitivity and/or molecular specificity for compound annotation. Some act as reactive matrices that introduce permanent charges and no longer require (de)protonation for ionization. However, OTCD side reactions are understudied, and it is presently unknown what pseudo metabolites can be generated as OTCD-derived artifacts. These are compounds that, in principle, exist as bona fide metabolites in tissues but that can also be products of OTCD side reactions. Here, it is demonstrated that besides expected reaction products, the reactive matrix 4-(anthracen-9-yl)-2-fluoro-1-methylpyridin-1-ium iodide (FMP)-10 can also cause unexpected *N*- and *O*-lactoylation and even apparent poly-lactoylation of multiple amino acids through Mukaiyama esterification. Side reactions are unrelated to MALDI laser photochemistry, as they happen in solution and can be readily observed by liquid chromatography–MS/MS. Since *N*-lactoylated amino acids have recently received much attention in sports physiology and obesity research, much care needs to be taken to distinguish true endogenous *N*-lactoylated amino acids from those that are formed by Mukaiyama side reactions.

1. Introduction

Mass spectrometry imaging (MSI), in particular matrix-assisted laser desorption/ionization (MALDI)-MSI, has become a mainstay technology in spatial biology, clinical research and pharmaceutical research and development.[1] The prominent role of MSI in spatially resolved biomedical research is not all that surprising, given its unique ability to enable spatially resolved visualization and structure elucidation of molecules as diverse as lipids, hydrophilic metabolites, drugs, drug metabolites, peptides, or N-glycans.[1] However, in current MALDI-MSI the "4S-parameters" for an ideal experiment,**s**peed,**s**ensitivity,**s**patial resolution, and**s**pecificity of compound annotations, often cannot be met at the same time.[1a] To get around some of these challenges, on-tissue chemical derivatization (OTCD) approaches and reactive matrices have been introduced in spatial peptidomics[2] and metabolomics (reviewed by.[3]) Derivatization has been used for a long time in liquid chromatography coupled to electrospray ionization MS (LC-ESI-MS) metabolomics, and chemical derivatization remains a field of active research.[4] Besides boosting sensitivity, for example, by addition of permanent charges, derivatization agents have been used to change the polarity of molecules,[5] stabilize molecular features like sialyl residues on glycans, which are strongly affected by in-source fragmentation,[6] or to differentiate isomeric structures.[6]

However, OTCD strategies require additional process steps and therefore come with additional challenges like delocalization and inefficient reaction conditions–especially in MSI.[3c] To reduce

T. Bausbacher, S. Schmidt, C. Hopf
Center for Mass Spectrometry and Optical Spectroscopy (CeMOS)
Mannheim University of Applied Sciences
Paul-Wittsack-Str. 10, 68163 Mannheim, Germany
E-mail: c.hopf@hs-mannheim.de

T. Bausbacher, C. Hopf
Mannheim Center for Translational Neuroscience (MCTN)
Heidelberg University
Ludolf-Krehl-Straße 13–17, 68167 Mannheim, Germany

A. L. Henneberg, C. A. Opitz
German Cancer Research Center (DKFZ), Heidelberg
Division of Metabolic Crosstalk in Cancer and the German Cancer Consortium (DKTK)
DKFZ Core Center Heidelberg
69120 Heidelberg, Germany

S. Meyer, A. K. Miller
Cancer Drug Development Group
German Cancer Research Center (DKFZ)
69120 Heidelberg, Germany

C. A. Opitz, C. Hopf
Medical Faculty
Heidelberg University
Im Neuenheimer Feld 672, 69120 Heidelberg, Germany

Supporting information for this article is available on the WWW under https://doi.org/10.1002/cmtd.202500090

metabolite delocalization in MALDI-MSI, the derivatization reagents are often dissolved in rather volatile solvents and subsequently sprayed onto a tissue section.[3,7] Hence, the duration for which a solvent-wet surface can extract, mix with, and react with the target molecules is often limited to only a few seconds. One way to increase reaction time and efficiency are incubation chambers with high humidity,[8] but these can cause increased delocalization especially of small polar molecules. To combat these challenges, modern derivatization reagents designed for MALDI-MSI are highly reactive, and some make use of additional activation agents.[9] A recently introduced and promising candidate is 4-(anthracen-9-yl)-2-fluoro-1-methylpyridin-1-ium iodide (FMP)-10.[7a] The molecule class features a 2-fluoro-*N*-alkylpyridinium salt with a positive charge to facilitate the derivatization and ionization, and an anthracene group to facilitate desorption in the MALDI process. FMP-10 was originally designed for MSI of neurotransmitters, where derivatization can take place at a primary or secondary amine group or at phenolic groups. In this context, side reactions in OTCD in general are rarely considered. Reactions of derivatization agents with themselves, with MALDI matrix and with unexpected functional groups have been noted.[10] However, the generation of "pseudo metabolites" by OTCD-induced conjugation of two true endogenous metabolites to form another true endogenous metabolite has not been described yet. Pseudo metabolites are broadly defined as false positives in metabolomics[11] that can be misannotations caused by lack of standards, in-source fragmentation or other reasons or be the result of sample preparation artifacts. Here, we narrowly define pseudo metabolites as compounds that can be enzymatically generated in tissues and therefore could be true metabolites but that are chemically generated during OTCD sample preparation instead. In this work, we describe the byproduct formation induced by derivatization of lactic acid and amino acids through a Mukaiyama esterification-like side reaction of FMP-10, thus highlighting the necessity that potential side reactions in OTCD need to be considered in quality assessment in MALDI imaging.[12]

N-lactoyl-phenylalanine (*N*-Lac-Phe) has recently been proposed as an exercise-inducible metabolite suppressing feeding and obesity,[13] as a metabolite mediating the drug action of metformin,[14] and as a putative biomarker and outcome parameter in patients with phenylketonuria.[15] Therefore, OTCD-induced *O*-linked lactoyl-amino acids could make MSI data interpretation a challenge in amino acid metabolism research. *N*-lactoyl-amino acids were first described in a biological context in 2015[16] and they have lately garnered much attention: Recent studies have highlighted the role of specific *N*-lactoyl amino acids, such as *N*-Lac-Phe as an appetite suppressant[13,14c] and a candidate mediator of diseases like obesity and type 2 diabetes.[14c] These findings suggest that *N*-lactoyl-amino acids may have substantial physiological and pharmacological roles.

2. Results and Discussion

We came across lactoyl amino acids rather serendipitously in a different biomedical context, namely brain metabolism and glioblastoma research: When applying FMP-10 OTCD on coronal mouse brain sections as well as to extracts of human U-87 MG glioblastoma cells (**Figure 1**a), we confirmed many of the neurotransmitters and their catabolites such as epinephrine, norepinephrine, homovanillic acid, 5-hydroxyindoleacetic acid (5-HIAA) or 3-methoxytyramine described in the original report of the reagent (Figure 1b).[7a] Surprisingly, we also observed signals corresponding to FMP-10-($C_{20}H_{14}N^+$)-derivatized Lac-Phe ($[M+C_{20}H_{14}N]^+$, *m/z* 505.212) and lactoyl-tyrosine (Lac-Tyr, $[M+C_{20}H_{14}N]^+$, *m/z* 521.207; Figure 1c,d). Aiming to confirm the identity of metabolites corresponding to these *m/z* values, we initially employed on-tissue MS/MS, but with very limited success. Only noise was detected when a small quadrupole isolation window ($m/z < 0.3$) was used, whereas with a bigger isolation window the spectra were dominated by fragments of coisolated small molecules. Despite poor spectral quality, the MS/MS spectra hinted at correct Lac-Tyr identification (Figure S1, Supporting Information). For more confident identification, we synthesized *N*-Lac-Tyr and *N*-Lac-Phe standards (Figure S2 to S7, Supporting Information) and used them for in-solution derivatization[17] followed by LC–MS/MS analysis (Figure 1a). As judged by comparable retention times (t_R) and MS/MS spectra of synthesized standards versus metabolite signals found in U-87 MG cell extracts, we identified low levels of *N*-Lac-Phe in the latter (Figure 1e). There, the extracted ion chromatogram (EIC) of *m/z* 505.212 (annotated as FMP-10-derivatized Lac-Phe [Lac-Phe+$C_{20}H_{14}N]^+$) presented two peaks with a retention time difference of 1.5 min (Figure 1e). The first peak ($t_R = 6.0$ min) matched the retention time ($\Delta\ t_R = 2.8$ s) of the synthesized *N*-Lac-Phe standard. In contrast, a ≈five times more intense second isobaric peak ($t_R = 7.5$ min) was only present in derivatized cell extract. Therefore, it was unlikely to represent Lac-Phe derivatized on a different functional group. In analogy, the EIC of *m/z* 521.207 ($[\text{Lac-Tyr}+C_{20}H_{14}N]^+$) featured only one peak in derivatized standard ($t_R = 4.6$ min), but two peaks in FMP-10-derivatized cell extract ($t_R = 4.6$ and 5.9 min; Figure 1f). For both *N*-Lac-Phe and *N*-Lac-Tyr, MS/MS fragmentation patterns of synthetic standards and the first peaks in derivatized cell extracts were identical (Figure 1g,h). Interestingly, lactoylation products of other molecules like neurotransmitters, which have already been described as substrates for FMP-10-derivatization in rodent brain, like serotonin and dopamine were observed as well (Figure S8, Supporting Information).

Fragmentation patterns of the cell extract-exclusive peak in EIC *m/z* 505.212 and an FMP-10-derivatized Phe standard were virtually identical, but the former displayed an additional neutral loss from the parent ion signal of $\Delta m/z$ 72 (Figure S10, Supporting Information). We hypothesized that this signal could represent a derivatization-induced condensation product between the carboxylic acid and hydroxyl groups of Phe and lactic acid, respectively, resulting in *O*-linked lactoylation. In support of this hypothesis, we detected a peak corresponding to double lactoylated Phe (*m/z* 577.233, Figure S10, Supporting Information). Its corresponding fragment spectrum showed two neutral losses of $\Delta m/z$ 72 as well as the Phe fragment signals. This finding suggested that derivatization-induced lactoylation may not only

Research Article
doi.org/10.1002/cmtd.202500090
Chemistry Europe
European Chemical Societies Publishing

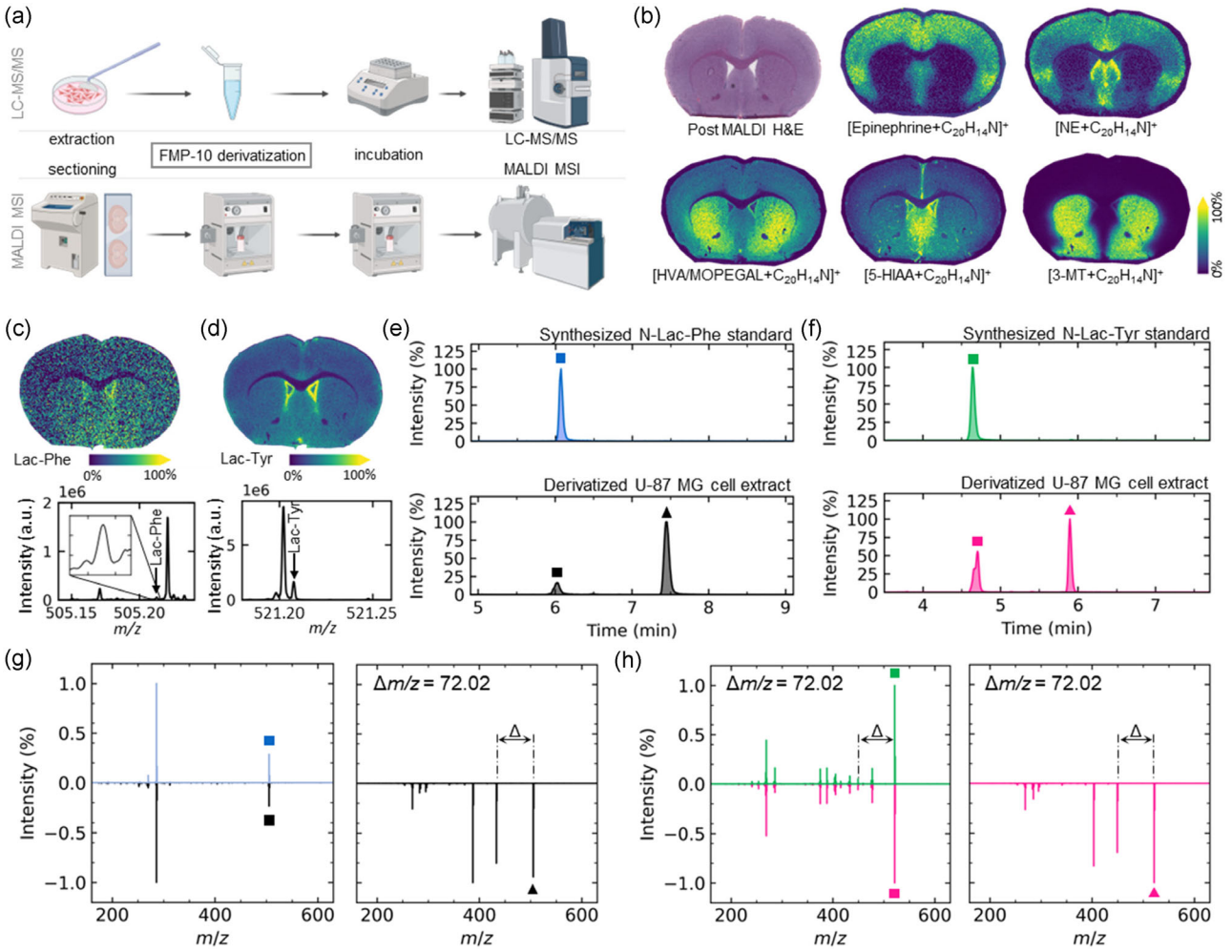

Figure 1. FMP-10-induced on-tissue generation of lactoyl-amino acids. a) Workflows for OTCD on mouse brain sections followed by MALDI-MSI (bottom) and for in-solution derivatization of U-87 MG glioblastoma cells with subsequent LC–MS/MS analysis (top). Created with https://BioRender.com/d23a134. b) Reference post-MALDI MS hematoxylin & eosin (H&E) histology staining and representative ion images of FMP-10-derivatized neurotransmitters previously described by Shariatgorji et al.[7a] using a modified protocol: *m/z* 451.2016 ($[M+C_{20}H_{14}N]^+$, epinephrine+FMP-10), *m/z* 437.1859 ($[M+C_{20}H_{14}N]^+$, norepinephrine (NE)+FMP-10), *m/z* 450.1699 ($[M+C_{20}H_{14}N]^+$, homovanillic acid (HVA)+FMP-10), *m/z* 459.1703 ($[M+C_{20}H_{14}N]^+$, 5-hydroxyindoleacetic acid (5-HIAA)+FMP-10), *m/z* 435.2067 ($[M+C_{20}H_{14}N]^+$, 3-methoxytyramine (3-MT)+FMP-10). Additional ion images in Figure S9, Supporting Information. c) Ion image of *m/z* 505.2121 ($[M+C_{20}H_{14}N]^+$; top), the theoretical mass of FMP-10-derivatized lactoyl-phenylalanine (Lac-Phe), as well as zoomed-in average spectrum of all MALDI MSI data points (bottom). d) Ion image of *m/z* 521.2074 ($[M+C_{20}H_{14}N]^+$; top), the theoretical mass of FMP-10-derivatized lactoyl tyrosine (Lac-Tyr), as well as zoomed-in average spectrum of all MALDI MSI data points (bottom). e) EIC of *m/z* 505.212 in FMP-10-derivatized synthetic *N*-Lac-Phe standard ($[M+C_{20}H_{14}N]^+$; blue square) or U-87 MG cell extract (black square and triangle). Squares indicate Lac-Phe, whereas triangle indicates an isobaric signal not found with synthetic standard. f) EIC of *m/z* 521.207 in FMP-10-derivatized synthetic *N*-Lac-Tyr standard ($[M+C_{20}H_{14}N]^+$; green square) or U-87 MG cell extract (pink square and triangle). Squares indicate Lac-Tyr, whereas triangle indicates an isobaric signal not found with synthetic standard. g) Left panel: MS/MS fragmentation patterns obtained for *N*-Lac-Phe standard (blue square) and an isobaric peak in FMP-10-derivatized U-87 MG cell extract (black square) that elutes at identical t_R. Right panel: Fragments of additional peak (isobaric to Lac-Phe; black triangle) exclusive to cell extract indicate that the parent ion is a distinctly different molecule and not FMP-10 reacting with a different functional group of Lac-Phe. Delta indicates the neutral loss of 72 Da (lactic acid). h) Left panel: MS/MS fragmentation patterns obtained for *N*-Lac-Tyr standard (green square) and an isobaric peak in FMP-10-derivatized U-87 cell extract (pink square) that elutes at identical t_R. Right panel: Fragments of additional peak (isobaric to *N*-Lac-Tyr; pink triangle) exclusive to cell extract.

apply to amino acids, but that lactic acid can be condensed to another lactic acid molecule and generate poly-lactic acid moieties.

Similarly, the cell extract-exclusive peak in EIC *m/z* 521.207 displayed the major fragments of FMP-10-derivatized Tyr with an additional neutral loss of *m/z* 72 from the parent ion signal (Figure S11, Supporting Information). Detection of a double lactoylated Tyr, as indicated by two neutral losses of *m/z* 72 from the parent ion, further supported the poly-lactoylation hypothesis (Figure S11, Supporting Information). Derivatization-induced esterification may not be limited to lactic acid. Indeed, we found initial evidence suggesting that also hydroxybutyric acid (HBA) may be conjugated to amino acids by indirect action of FMP-10. Analogous to lactoylated Phe and Tyr, we observed chromatographic peaks for the *m/z* of FMP10+Tyr+HBA and FMP10+Phe+HBA, MS/MS spectra of which displayed all fragments characteristic for derivatized Tyr and Phe and that additionally featured a neutral loss from the parent ion of 86 Da (Figure S12, Supporting Information).

Research Article
doi.org/10.1002/cmtd.202500090
Chemistry Europe
European Chemical Societies Publishing

This unexpected result suggested that FMP-10 could promote lactic acid polymerization and react with poly lactic acid. Indeed, ion images corresponding to lactic acid polymers with chain lengths of two and three were detected (**Figure 2**a) and show considerable colocalization with ion images corresponding to derivatized Tyr and Lac-Tyr or Phe and Lac-Phe, especially in the lateral ventricular area (Figure S13, Supporting Information). To gain more mechanistic understanding, we performed a substructure search with FMP-10 and looked into esterification and condensation reactions. We noticed that the reactive 2-fluoro-*N*-methyl-pyridine scaffold of FMP-10 bears striking resemblance with Mukaiyama salts. FMP-10 is therefore likely to have similar reactivity as other 2-halo-*N*-alkylpyridinium salts including the Mukaiyama reagent, which is commonly used as a condensation reagent in organic synthesis[18] (Figure 2b).

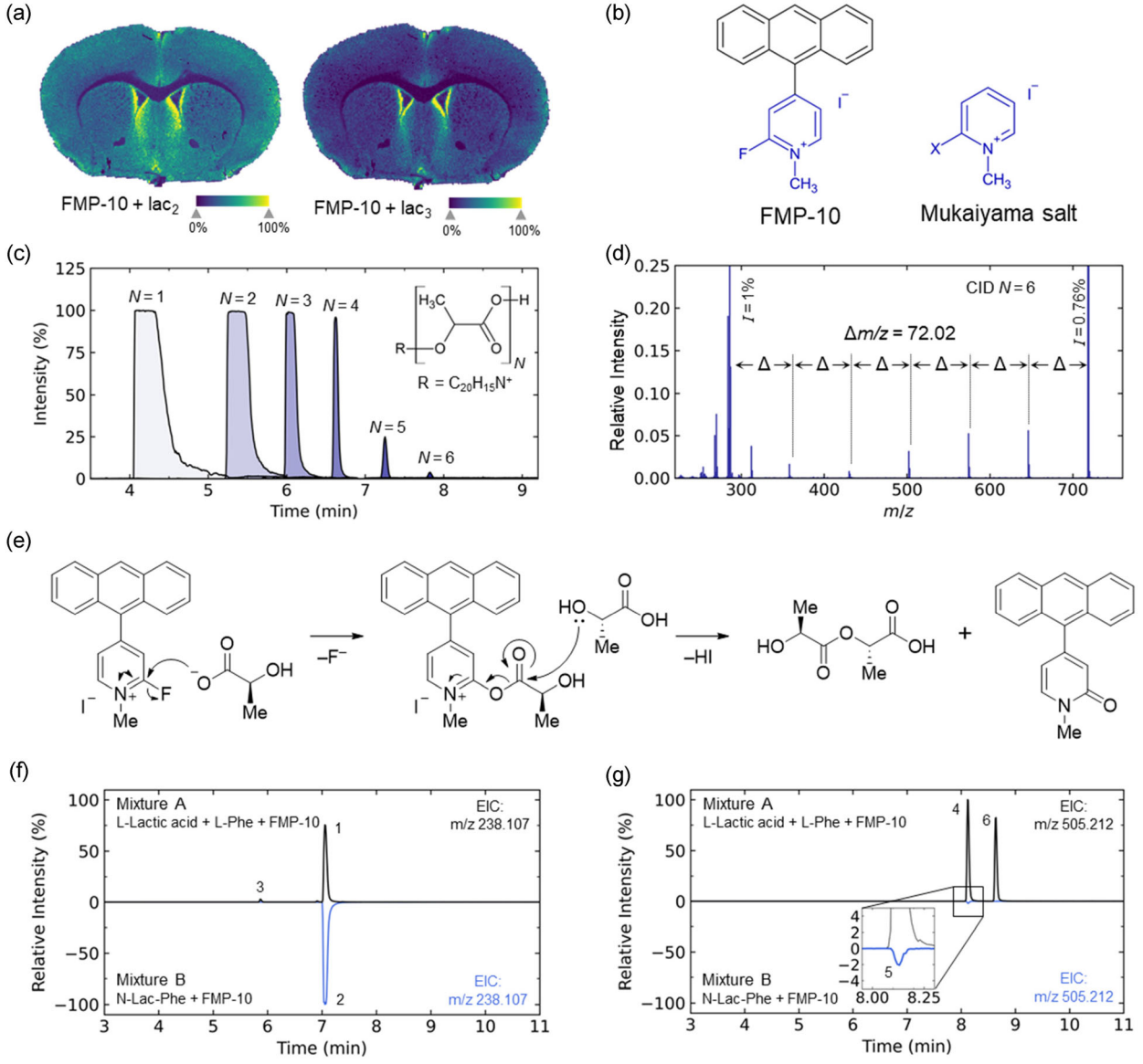

Figure 2. FMP-10 induces condensation reactions during OTCD and in-solution derivatization. a) Ion images indicating the spatial distribution of *m/z* 430.165 ($[M+C_{20}H_{14}N]^+$, corresponding to FMP-10 + 2x lactic acid; ±1 ppm) and *m/z* 502.187 ($[M+C_{20}H_{14}N]^+$, i.e., FMP-10 + 3x lactic acid; ±1 ppm) in mouse brain tissue sections following OTCD. *m/z* of molecular ions correspond well to the theoretical mass of FMP-10-derivatized poly lactic acid with chain lengths of 2 and 3. b) Chemical structure of FMP-10 and a representative structure for a Mukaiyama salt. Marked in blue are substructures that are similar in both molecules. X denotes any halogen atom. c) In-solution derivatization of FMP-10 with lactic acid: EICs for *m/z*: 358.143 (N = 1), 430.165 (N = 2), 502.187 (N = 3), 574.207 (N = 4), 646.228 (N = 5), 718.249 (N = 6) representing FMP-10-derivatized poly lactic acid chains with repeating units of N = 1 to 6. d) Fragmentation patt ern of parent ion *m/z* 718.248 ($[M + C_{20}H_{14}N]^+$, N = 6). Neutral loss Δ*m/z* of 72.02 is indicated. e) Proposed reaction mechanism for the extension of the poly lactic acid chains induced by FMP-10. f) In-solution derivatization of L-lactic acid and L-phenylalanine (Mixture A, top) and *N*-Lac-Phe (Mixture B, bottom). Shown are EICs of *m/z* 238.107 in both mixtures representing the theoretical mass of underivatized Lac-Phe ($[M+H]^+$). Retention times (RT) of three chromatographic peaks: 1, 7.05; 2, 7.1; 3, 5.87 min. Fragmentation spectra of each peak are shown in Figure S16, Supporting Information. The cosine similarity score between fragmentation spectra of peak 1 and peak 2 was 0.995. g) In-solution derivatization of L-lactic acid and L-phenylalanine (Mixture A, top) and *N*-Lac-Phe (Mixture B, bottom). Shown are EICs of *m/z* 505.2122 in both mixtures representing the theoretical mass of derivatized Lac-Phe ($[M]^+$). RT of chromatographic peaks: 4, 8.12; 5, 8.1; 6, 8.64 min. Fragmentation spectra of each peak are shown in Figure S16, Supporting Information. Cosine similarity score between fragmentation spectra of peak 4 and peak 5 was 0.997.

To explore FMP-10-induced lactic acid polymerization further, we went back to in-solution reactions and LC–MS/MS analysis: Since only polymers with chain lengths of two and three were detected in MALDI-MSI, we hypothesized that the degree of polymerization may be influenced by the interaction time between FMP-10 and lactic acid in the sample. In MALDI-MSI, the derivatization reagent is applied using a pneumatic sprayer and, consequently, a wet environment needed for an efficient reaction, is present for only a few seconds per spraying cycle. In contrast, the in-solution derivatization process involves heating and shaking of the reaction mixture for 30 min, providing optimal reaction conditions that may lead to higher degrees of lactic acid polymerization. Under these conditions, we identified a series of peaks with *m/z* differences of N = 1–6 multiples of 72 whose MS/MS spectra mainly comprised the fragment of FMP-10 and neutral losses of 72 (Figure 2c,d, Figure S14, Supporting Information). We identified these signals as lactic acid polymers.

Lactic acid polymers have not been described as endogenous molecules in the literature, suggesting that they were derivatization-induced. These findings further support our hypothesis that FMP-10 derivatization can induce poly-lactoylation in biological samples. Lactic acid is a ubiquitous and abundant molecule in biological samples. Its concentration ranges from 1.5 to 3 mM under normal physiological conditions and can reach 10–40 mM in inflammatory environments or the tumor microenvironment.[19] Similarly, amino acids are ubiquitous in mammalian cells.[20] In addition to ester formation, Mukaiyama salts have demonstrated utility in amide bond synthesis.[21] This suggests that beyond the lactic acid condensation with alcohols or carboxylic acid groups described here, Mukaiyama amide formation between amines and lactic acid or other carboxylic acids are likely. To test this hypothesis, we set up a simple FMP-10 in-solution derivatization of A: L-lactic acid and L-phenylalanine standards and B: N-Lac-Phe. Indeed, sample A produced chromatographic peaks with identical retention time and fragmentation spectra to underivatized *N*-Lac-Phe (Figure 2f, peak 1 and 2) and derivatized *N*-Lac-Phe (Figure 2g, peak 4 and 5). Additionally, sample A also produced chromatographic peaks for what appears to be underivatized (Figure 2f, peak 3) and derivatized (Figure 2g, peak 6) O-linked Lac-Phe. No peak was found at the corresponding RT in sample B. Furthermore, multiple additional condensation products were detected in condensations between two *N*-Lac-Phe- and two Phe molecules (Figure S15, Supporting Information).

In analogy with a published reaction mechanism of Mukaiyama salts,[18] we propose a possible reaction mechanism for lactate polymerization or lactate conjugation with amino acids (Figure 2e). Consequently, even though we confirmed that *N*-lactoyl amino acids were present in the processed sample by employing a synthetic standard, the abundance of the educts of the lactic acid to amino acid condensation reaction suggests that possibly reasonable amount of the signal detected in OTCD in MALDI imaging and the in-solution derivatization approach was a product of FMP-10 derivatization and not an endogenous metabolite. Ultimately, assumptions regarding the presence or quantity of lactoylated amino acids or other esterification or amide products using FMP-10 derivatization should be approached with caution, and derivatization results require thorough evaluation and careful interpretation.

3. Conclusion

Our study presents the first observation and characterization of an undesired side reaction occurring between lactic acid and amino acids, as well as between lactic acid molecules themselves, when using derivatization protocols involving 2-halo-*N*-alkylpyridinium salts. We discovered that *O*-lactoylated amino acids as well as *N*-lactoylated amino acids, which currently attract much attention as true physiologically important metabolites, can be produced as a result of this side reaction. Consequently, these derivatization protocols should be used with great caution and validated by complementary methods without derivatization.

4. Experimental Section

Materials, Tissues, Equipment, and Software: Tissues, Cells, and Materials

Fresh-frozen brains from naïve male C57BL/6 mice were purchased from Heidelberg Pharma AG (Ladenburg). U-87 MG malignant glioma cells were obtained from ATCC (Manassas, Virginia, USA).

All reagents were purchased at the highest level of purity and used without further purification. Indium-tin oxide (ITO)-coated glass slides (Bruker Daltonics, Bremen, Germany), acetonitrile (Honeywell, Charlotte, North Carolina, USA), water (VWR, Radnor, Pennsylvania, USA), methanol (Honeywell), formic acid (VWR), FMP-10 (Tag-ON AB, Uppsala, Sweden), l-tyrosine (Carl Roth, Karlsruhe, Germany), l-phenylalanine (Sigma Aldrich Chemie, Taufkirchen, Deutschland), Dulbecco's modified Eagles medium (DMEM, Life Technologies, Darmstadt, Germany), fetal bovine serum (FBS, Life Technologies), l-glutamine (Sigma-Aldrich), sodium pyruvate (Life Technologies GmbH), penicillin–streptomycin (Life Technologies), phosphate-buffered saline (PBS, Life Technologies), l-lactic acid (Sigma-Aldrich), hexafluorophosphate benzotriazole tetramethyl uranium (BLDpharm, Reinbek, Germany), dichloromethane, *N*,*N*-diisopropylethylamine (Carl Roth), $CDCl_3$, D_2O, ethyl acetate, l-phenylalanine ethyl ester hydrochloride (Thermo Scientific Chemicals), and l-tyrosine ethyl ester hydrochloride (Thermo Scientific Chemicals).

For chemical synthesis, reagents were purchased at the highest level of purity and used without further purification. Stabilized THF (synthesis grade) and anhydrous CH_2Cl_2 (prepared with an MBraun SP system) were used for reactions. EtOAc and *n*-heptanes were purchased as HPLC grade and MeOH as P.A. grade. All reactions were magnetically stirred. Analytical thin-layer chromatography (TLC) was performed on Merck glass silica plates coated with a fluorescent indicator F_{254}. Spots were visualization with 254 nm UV light and a basic $KMnO_4$ stain with heating.

Acclaim RSLC 120 C18 2 µm 2.1 × 150 mm Thermo Fisher Scientific, Dreieich, Germany), ACQUITY UPLC HSS T3 Column, 100 Å, 1.8 µm, 2.1 × 150 mm (Waters, Eschborn, Germany), Slide box (neoLab, Heidelberg, Germany), Vacuum sealer and foil (CASO, Arnsberg, Germany), Centrifuge (Heraeus Fresco 21, Thermo Fisher Scientific), Vacuum concentrator (Concentrator plus, Eppendorf SE, Hamburg Germany), Vacuum desiccator (SP Bel-Art, Wayne, New Jersey, USA).

Types of Equipment and Software

A Solarix XR 7 T (Bruker Daltonics) equipped with a Smartbeam-II Nd:YAG laser (355 nm) was used for the acquisition of all MALDI MSI and on-tissue MS/MS data. Reactive FMP-10 matrix was applied using an M5 pneumatic sprayer (HTX Technologies LLC, Chapel Hill, North Carolina, USA). LC–MS/MS data acquisition was performed on an Elute UHPLC system (Bruker Daltonics) connected to a timsTOF flex mass spectrometer (Bruker Daltonics). MALDI MS data analysis was performed using DataAnalysis 6.1 and SCiLS Lab 2024 (Bruker Daltonics). Frozen mouse brain tissue was sectioned using a Leica CM1850 cryostat (Leica Biosystems, Nussloch, Germany). Optical images were recorded with an Aperio CS2 Scanner (Leica Biosystems). Analytical LC/MS was performed on an Agilent 1260 Infinity system equipped with a 6120 Quadrupole mass detector and evaporative light scattering detector. UV-detection at 210–500 nm in 4 nm steps. Medium pressure column chromatography was performed with a RediSep Rf system (Teledyne Isco) and RediSep Rf columns (Teledyne Isco). High resolution mass spectrometry (HRMS) was recorded on a Bruker ApexQe Fourier-transform ion cyclotron resonance (FT-ICR) instrument. NMR spectra were recorded on a Bruker Avance III 9.4 T operating at 400 MHz for ^{1}H nuclei and 100 MHz for ^{13}C nuclei. Spectra were recorded at 298.1 K. Spectra were referenced to the solvent signal ($CDCl_3$: ^{1}H = 7.26 ppm, ^{13}C = 77.16 ppm; D_2O: ^{1}H = 4.79 ppm; CD_3OD: ^{1}H = 3.31 ppm, ^{13}C = 49.0 ppm). Spectra were analyzed in MestReNova 14.3.0 (Bajo Santiago de Compostela, Spain).

MALDI MS Imaging: Sample Preparation

Frozen mouse brains were cut into 12 μm thick sections and mounted onto ITO-coated glass slides (Bruker Daltonics), stored in slide boxes, covered and vacuum-sealed in foil (CASO, Arnsberg, Germany), and stored at –80 °C until further processing. Immediately before OTCD or matrix coating, frozen slides were equilibrated at room temperature (RT), removed from vacuum-sealed foil and dried for 10 min in a vacuum desiccator (SP Bel-Art).

FMP-10 OTCD

Reactive FMP-10 matrix was applied in two steps according to a published protocol[7a,22] with the following modifications. FMP-10 step: 10 mg of FMP-10 was dissolved in 5.5 mL of 70% ACN in water (v/v) and sprayed onto the tissue sections. Incubation step: only 70% ACN in water (v/v) was sprayed.

Parameter	FMP-10	Incubation
Nozzle temperature [°C]	60	50
Number of passes	20	20
Concentration [mg mL^{-1}]	1.82	0
Flow rate [mL min^{-1}]	0.08	0.12
Velocity [mm min^{-1}]	1100	1200
Track spacing [mm]	2	2
Pattern	CC	CC
Pressure [psi]	10	10
Gas flow rate	2	2
Dry time [s]	0	0
Nozzle height [mm]	40	40

Magnetic Resonance MALDI MS Imaging Data Acquisition

MSI Data was acquired on a 7T FT-ICR mass spectrometer (solariX XR 7T, Bruker Daltonics). To reduce matrix background and the overall ion load in the ICR cell, a CASI window of 113 Da around *m/z* 473 was used, reducing the effective *m/z* range to 425–525. Peak filtering was set to SNR >3 and an absolute intensity threshold of 10^5 arbitrary units (a.u.). A data reduction factor of 95% was applied. The *m/z* range 247–800 at a transient size of 2 M resulted in a free induction decay of 2.41 s and a theoretical mass resolving power of 320 k at *m/z* 400. A matrix signal at *m/z* 523.2169 ($C_{39}H_{27}N_2^+$) was used for single point online calibration. Profile data was imported into SCiLS Lab 2024 Pro software (Bruker Daltonics) and root mean square (RMS)-normalized. Raw spectra were evaluated in DataAnalysis software (Bruker Daltonics), and the smart formula function was used to generate sum formulae. Unless otherwise stated, ion images are shown as $[M+C_{20}H_{14}N]^+$ to account for the mass added by FMP-10.

Synthesis of *N*-Lactoylated Phe (N-Lac-Phe) and *N*-Lactoylated Tyr (N-Lac-Tyr)

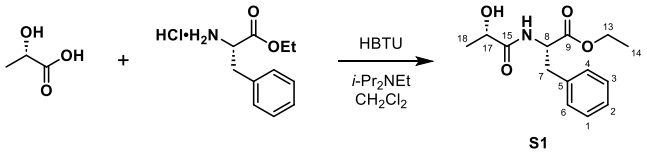

S1

Ethyl ((*S*)-2-Hydroxypropanoyl)-*L*-Phenylalaninate (S1):

According to a procedure by Long et al.[13] to a solution of l-lactic acid (1.62 g, 18.0 mmol, 1.0 eq.) in anhydrous CH_2Cl_2 (90 mL) was added HBTU (8.19 g, 21.6 mmol, 1.2 eq.) under argon. After 15 min at room temperature, a solution of l-Phe-OEt•HCl (4.13 g, 18.0 mmol, 1.0 eq.) and *i*-Pr_2NEt (6.98 g, 54.0 mmol, 3.0 eq.) in CH_2Cl_2 (90 mL) was added dropwise. After 18 h, the reaction mixture was washed with 0.1 M aqueous HCl (2 × 50 mL), 5% aqueous $NaHCO_3$ (2 × 50 mL), and brine (2 × 50 mL), dried ($MgSO_4$), filtered, and concentrated in vacuo. The product was purified by medium pressure LC (40% EtOAc in *n*-heptane) to yield S1 as a yellowish oil (2.23 g, 8.42 mmol, 47%).

TLC R_f = 0.29 (40% EtOAc in *n*-heptane)

LC/MS (ESI) *m/z*: 266.1, 288.1; t_R = 4.0 min

^{1}H NMR (400 MHz, $CDCl_3$) δ 7.31–7.21 (m, 3H, C^{Ar}), 7.15–7.09 (m, 2H, C^{Ar}), 6.90 (br d, 1 H, NH), 4.85 (dt, *J* = 8.3 Hz, *J* = 6.1 Hz, 1H, H-C8), 4.26–4.19 (m, 1H, H-C17), 4.17 (dq, *J* = 7.2 Hz, *J* = 0.5 Hz, 2H, H-C13), 3.18 (dd, *J* = 13.9, 5.9 Hz, 1H, H^A-C7), 3.09 (dd, *J* = 13.9, 6.3 Hz, 1H, H^B-C7), 1.34 (d, *J* = 6.8 Hz, 3H, H-C18), 1.24 (d, J = 7.1 Hz, 3H, H-C14) ppm

^{13}C NMR (101 MHz, $CDCl_3$) δ 174.2 (C15), 171.7 (C9), 135.9 (C5), 129.4 (C4, C6), 128.7 (C1, C3), 127.3 (C2), 68.5 (C17), 61.8 (C13), 52.8 (C8), 38.1 (C7), 21.2 (C18), 14.2 (C14) ppm

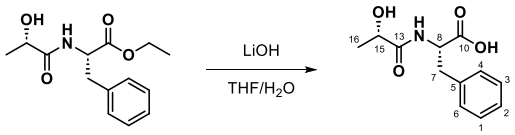

S1 Lac-Phe

((*S*)-2-hydroxypropanoyl)-*L*-phenylalanine (N-Lac-Phe):

To a solution of S1 (2.23 g, 8.42 mmol, 1.0 eq.) in THF (17 mL) was added a solution of LiOH (403.3 mg, 16.84 mmol, 2.0 eq.) in H_2O

(34 mL) dropwise at room temperature. After 2 h, the solvent was removed in vacuo and the resulting residue was diluted with EtOAc (100 mL) and H_2O (100 mL). The aqueous layer was acidified to pH 3 with 1 M HCl and the mixture was stirred until all solids had dissolved. The two layers were separated and the aqueous layer was extracted with EtOAc (2 × 50 mL). The combined organic layers were washed with brine (50 mL), dried ($MgSO_4$), filtered, and concentrated in vacuo. The product was purified by crystallization from a hot EtOAc/*n*-heptane mixture. The resulting crystals were filtered onto a sintered-glass funnel, washed with an ice-cold EtOAc/*n*-heptane mixture (2 × 25 mL), then room temperature *n*-heptane (2 × 25 mL), and dried under high vacuum to give **N-Lac-Phe** as white crystals (1.36 g, 5.77 mmol, 69%).

Melting point: 128.3–128.8 °C

LC/MS (254 nm) $t_R = 3.2$ min, 99% purity

^{1}H NMR (400 MHz, D_2O) δ 7.41–7.26 (m, 5H, H-C_{Ar}), 4.72 (dd, $J = 9.1$ Hz, $J = 5.2$ Hz, 1H, H-C8), 4.18 (q, $J = 6.9$ Hz, 1H, H-C15), 3.30 (dd, $J = 13.9$ Hz, $J = 5.2$ Hz, H^A-C7), 3.06 (dd, $J = 13.9$ Hz, $J = 9.1$ Hz, 1H, H^B-C7), 1.18 (d, $J = 6.9$ Hz, 3H, H-C16) ppm

^{13}C NMR (101 MHz, D_2O) δ 180.1 (C13), 177.7 (C10), 139.4 (C^{Ar}), 132.2 (C^{Ar}), 131.6 (C^{Ar}), 130.0 (C^{Ar}), 70.4 (C15), 56.2 (C8), 39.5 (C7), 22.3 (C16) ppm

HRMS (ESI) *m/z*: $[M+Na]^+$ calc. for $C_{12}H_{15}NNaO_4^+$: 260.0893; found: 260.0895

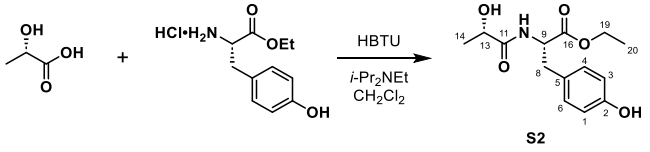

Ethyl ((*S*)-2-hydroxypropanoyl)-*L*-tyrosinate (S2):

To a solution of l-lactic acid (1.35 g, 15.0 mmol, 1.0 eq.) in anhydrous CH_2Cl_2 (75 mL) was added HBTU (6.83 g, 18.0 mmol, 1.2 eq.) under argon. After 15 min at room temperature, a solution of l-Tyr-OEt•HCl (3.69 g, 15.0 mmol, 1.0 eq.) and *i*-Pr_2NEt (5.82 g, 45.0 mmol, 3.0 eq.) in CH_2Cl_2 (75 mL) was added dropwise. After 18 h, the reaction mixture was washed with 0.1 M aqueous HCl (2 × 100 mL), 5% aqueous $NaHCO_3$ (2 × 100 mL), and brine (2 × 100 mL), dried ($MgSO_4$), filtered, and concentrated in vacuo. The product was purified by medium pressure LC (75% EtOAc in *n*-heptane) to S2 as a light-yellow oil (1.79 g, 6.39 mmol, 43%).

TLC R_f = 0.42 (75% EtOAc in *n*-heptane)

LC/MS (ESI) *m/z*: 282.1, 304.1; $t_R = 3.4$ min

^{1}H NMR (400 MHz, $CDCl_3$) δ 7.79–7.66 (m, 1H, OH), 7.15 (d, $J = 8.7$ Hz, 1H, NH), 7.00–6.89 (m, 2H, H-C4, H-C6), 6.79–6.65 (m, 2H, H-C3, H-C1), 4.89–4.69 (m, 1H, H-C9), 4.17 (q, $J = 7.2$ Hz, 2H, H-C19), 4.13–4.06 (m, 1H, H-C13), 3.87 (s, 1H, OH), 3.08 (dd $J = 14.0$ Hz, $J = 5.5$ Hz, 1H, H^A-C8), 2.96 (dd, $J = 14.0$ Hz, $J = 6.8$ Hz, 1H, H^B-C8), 1.30–1.19 (m, 6H, H-C14, H-C20) ppm

^{13}C NMR (101 MHz, $CDCl_3$) δ 175.1 (C11), 172.1 (C16), 155.8 (C2), 130.4 (C4), 126.8 (C5), 115.7 (C3), 68.4 (C13), 61.9 (C19), 52.9 (C9), 37.3 (C8), 20.9 (C14), 14.2 (C20) ppm

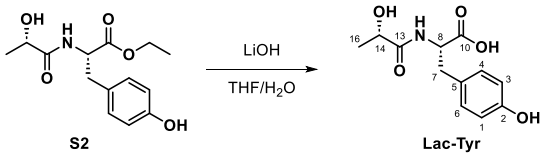

((*S*)-2-hydroxypropanoyl)-*L*-tyrosine (N-Lac-Tyr):

To a solution of S2 (1.79 g, 6.39 mmol, 1.0 eq.) in THF (14 mL) was added a solution of LiOH (306 mg, 12.8 mmol, 2.0 eq.) in H_2O (24 mL) dropwise at room temperature. After 2 h, the solvent was removed in vacuo and the resulting residue was diluted with EtOAc (100 mL) and H_2O (100 mL). The aqueous layer was acidified to pH 3 with 1 M HCl and the mixture was stirred until all solids had dissolved. The two layers were separated and the aqueous layer was extracted with EtOAc (2 × 50 mL). The combined organic layers were washed with brine (50 mL), dried ($MgSO_4$), filtered, and concentrated in vacuo. The product was purified by crystallization from a hot EtOAc/*n*-heptane mixture. The resulting crystals were filtered onto a sintered-glass funnel, washed with an ice-cold EtOAc/*n*-heptane (2 × 25 mL), then room temperature *n*-heptane (2 × 25 mL), and dried under high vacuum to give **N-Lac-Tyr** as white crystals (472 mg, 1.86 mmol, 29%).

Melting point 156.5–156.9 °C

LC/MS (254 nm) $t_R = 2.6$ min, 99% purity

^{1}H NMR (400 MHz, D_2O) δ 7.17–7.11 (m, 2H, H-C^{Ar}), 6.87–6.81 (m, 2H, H-C^{Ar}), 4.66 (dd, $J = 9.0$ Hz, $J = 5.2$ Hz, 1H, H-C8=), 4.18 (q, $J = 6.9$ Hz, 1H, H-C14), 3.20 (dd, $J = 14.1$ Hz, J =5.2 Hz, 1H, H^A-C7), 2.97 (dd, $J = 14.1$, 9.0 Hz, 1H, H^B-C7), 1.18 (d, $J = 6.9$ Hz, 3H, H-C16) ppm

^{13}C NMR (101 MHz, D_2O) δ 180.0 (C13), 177.7 (C10), 157.3 (C2), 133.5 (C4), 131.2 (C5), 118.3 (C3), 70.5 (C14), 56.3 (C8), 38.7 (C7), 22.3 (C16) ppm

HRMS (ESI) *m/z*: $[2M+Na]^+$ calc. for $C_{24}H_{30}N_2NaO_{10}^+$: 529.1793; found: 529.1797

Cell Treatment and LC–MS/MS Analysis of Metabolites: Cell Treatment and Sample Preparation

U-87 MG malignant glioma cells were seeded in 6 cm dishes at a cell density of 8×10^5 cells/dish, and the medium (DMEM with 4.5 g L^{-1} glucose, supplemented with 10% FBS, 2 mM L-glutamine, 1 mM sodium pyruvate, 100 U mL^{-1} penicillin, and 100 µg mL^{-1} streptomycin) was refreshed 24 h after seeding. After 72 h in culture, cells were washed twice with ice-cold PBS and 1 mL of ice-cold 80% MeOH was added. After 20 min of incubation at −80 °C, cells were scraped and transferred into new reaction tubes. Cells were homogenized by vigorous vortexing and sonication for 5 min prior to centrifugation at full-speed for 10 min in a precooled centrifuge. In parallel, the synthesized N-Lac-Phe and N-Lac-Tyr, along with standards of Tyr and Phe were each dissolved in 50% ACN to a concentration of 1 mM. The standard solutions were combined and diluted in 50% ACN to a final concentration of 100 µM. Samples and 1 mL of standard solution were dried in a cooled vacuum concentrator and reconstituted in 200 µL of 70% ACN, followed by vortexing and sonication for 10 min. Subsequently, 500 µL of a 1 mg mL^{-1} solution of FMP-10 in ACN was added, and the mixture was incubated at 40 °C with shaking for 30 min. To terminate the reaction, 500 µL of methanol was added, and the samples were dried again using a vacuum concentrator. Finally, the samples were redissolved in 500 µL of 50% ACN in water. After vortexing and sonication for an additional 10 min, the samples were analyzed.

FMP-10 Induced Condensation Reaction Using Lactic Acid and Phenylalanine Standards

Four mixtures of standards (200 µl) were set up. Sample A: 5 mM L-phenylalanine, 10 mM L-lactic acid; Sample B: 5 mM N-Lac-Phe;

Sample A control: 5 mM L-phenylalanine, 10 mM L-lactic acid; Sample B control: 5 mM N-Lac-Phe. 600 µl of a 1 mg mL^{-1} solution of FMP-10 in ACN was added to sample A and B. 600 µl of ACN was added to samples A control and B control. All following steps were performed identically on all samples. Samples were shaken at 40 °C for 30 min and 500 µL of methanol was added to quench the reaction. Afterward, samples were dried under gentle nitrogen flow for around 3 h until completely dry. 500 µL of 35% ACN was used to reconstitute the samples before injection into the LC–MS system.

LC–MS/MS Data Acquisition for Derivatized Cell Extracts

LC–MS/MS was performed on an Elute UHPLC system coupled with a timsTOF Flex mass spectrometer. Mobile phase A consisted of 0.1% formic acid in water, while phase B consisted of 0.1% formic acid in ACN. Chromatography used a 150 mm Acclaim RSLC 120 C18 column (particle size of 2.2 µm, pore size of 120 Å, inner diameter of 2.1 mm). Gradient elution (0.4 mL min^{-1} flow rate): 20% to 80% B over 8.5 min, followed by 100% B for 1.5 min, and reequilibration at 10% B for 2 min. The injection volume for each sample was set at 2 µL.

Data was acquired in positive ion mode across an *m/z* range of 50–1300, with a scan speed of 12 Hz. The acquisition window was divided into three segments with identical MS settings: The first segment (0 to 0.03 min) was a standby segment where only MS1 data was recorded, and the LC flow was directly coupled to the MS system. The second segment (0.03 to 0.3 min) served as a recalibration segment, where only MS1 data was recorded while the LC flow was diverted through an external sample loop filled with sodium formate before reaching the MS system. The external sample loop was filled by a syringe pump during segment three, in which the LC flow was once again directly connected to the MS system for actual data acquisition using the following parameters

Parameter general MS	
Deflection 1 delta [V]	60
Funnel 1 RF [Vpp]	300
Funnel 2 RF [Vpp]	300
Multipole RF [Vpp]	300
Collision energy in MS1 [eV]	1
Collision RF [Vpp]	2000
Quadrupole ion energy [eV]	5
Low mass [m/z]	390
TOF transfer time [µs]	100
TOF pre pulse storage [µs]	5
Focus mode	On
Sweeping	On
Parameter auto MS	
Total cycle time [s]	0.5
MS/MS rate control	Dynamic
MS/MS target intensity	25,000
MS/MS spectra rate limits [Hz]	16–30
MS/MS exclusion range [m/z]	50–300
Active exclusion after X spectra	3
Exclude for X minutes	0.2

A four-segment sweeping mode was used. Consequently, every scan was recorded four times with different parameter sets each time. Set 1: collision RF 1000 Vpp, TOF transfer time 50 µs, collision energy 100% (20 eV); Set 2: collision RF 1000 Vpp, TOF transfer time 50 µs, collision energy 250% (50 eV); Set 3: collision RF 2000 Vpp, TOF transfer time 100µs, collision energy 100% (20 eV); Set 4: collision RF 2000 Vpp, TOF transfer time 100 µs, collision energy 250% (50 eV). The base collision energy was set to 20 eV.

LC–MS/MS Data Acquisition for in Solution Derivatization of Lactic Acid and Phe

Data acquisition was performed very similarly to 4.3 with the following changes. Low mass *m/z* was adjusted to *m/z* 90. Separation was performed on a Waters ACQUITY HSS T3 column (2.1 × 150 mm) using the following gradient: 5% to 10% B over 3 min, 10% to 60% B over 4 min, 60& to 80% B over 3.5 min, followed by 2.5 min at 95% B. Reequilibration was performed for 3 min at 5% B.

Data Analysis and Visualization

MALDI MSI data was visualized using SCiLSLab 2024. Shortly, centroided data was imported and RMS-normalized. Ion images of the theoretical *m/z* values of proposed molecules were visualized using an *m/z* window of 2 ppm and a hotspot removal of 99%. LC–MS/MS data was visualized using DataAnalysis 6.1. Neutral loss filtering was performed in Metaboscape 2024 (all software from Bruker Daltonics).

Acknowledgements

The authors thank Lars Gruber and Qiuqin Zhou for helpful discussions, and Livia von Ammon for the sectioning of mouse brain tissue. Funding for this study was kindly provided by the Deutsche Forschungsgemeinschaft (DFG) for SFB 1389 UNITE-Glioblastoma (project 404521405 to C.A.O. and C.H), by the Ministry of Science and Arts Baden-Württemberg (MWK Mittelbauprogramm to C.H.) and by German Federal Ministry of Education and Research (BMBF) for project DrugsData (grant 13FH8I09IA to C.H.) of the innovation partnership M^{2}Aind within the framework FH-Impuls. The authors acknowledge funding from the TALETE project (FKZ 01KT2315) that is supported by the German Federal Ministry of Education and Research (BMBF) and the EC under the framework of the ERA-NET TRANSCAN-3 Initiative to A.L.H. and C.A.O. Funding to S.M. was provided by a DKFZ postdoctoral fellowship.

Open Access funding enabled and organized by Projekt DEAL.

Conflict of Interest

The authors declare no conflict of interest.

Author Contributions

Tobias Bausbacher: conceptualization (equal); data curation (lead); formal analysis (lead); investigation (lead); methodology (lead); project administration (supporting); validation (lead); visualization (lead); writing—original draft (equal); writing—review & editing (supporting). **Alessa L. Henneberg**: conceptualization (supporting); project administration (supporting); validation

(supporting); writing—review & editing (supporting). **Stephanie Meyer**: conceptualization (supporting); formal analysis (supporting); investigation (supporting); methodology (supporting); validation (supporting); writing review & editing (supporting). **Stefan Schmidt**: project administration (supporting); supervision (supporting); visualization (supporting); writing—review & editing (supporting). **Aubry K. Miller**: conceptualization (equal); data curation (supporting); formal analysis (equal); methodology (supporting); resources (supporting); supervision (supporting); writing—review & editing (supporting). **Christiane A. Opitz**: conceptualization (equal); funding acquisition (equal); methodology (supporting); project administration (supporting); resources (equal); supervision (equal); writing—original draft (supporting); writing—review & editing (supporting). **Carsten Hopf**: conceptualization (equal); funding acquisition (equal); methodology (equal); project administration (equal); resources (equal); supervision (equal); writing original draft (equal); writing—review & editing (equal). **Aubry K. Miller**, **Christiane A. Opitz**, and **Carsten Hopf** contributed equally to this work.

Data Availability Statement

All MALDI MSI data is available through the Metaspace portal (https://metaspace2020.org/project/bausbacher-2025). Raw data has been deposited in Zenodo under accession code https://doi.org/10.5281/zenodo.17046760.

Keywords: FMP-10 · lactoylated amino acids · matrix-assisted laser desorption/ionization imaging · on-tissue chemical derivatization · side reactions

[1] a) S. Schulz, M. Becker, M. R. Groseclose, S. Schadt, C. Hopf, *Curr. Opin. Biotechnol.* **2019**, *55*, 51. b) M. E. Colley, A. B. Esselman, C. F. Scott, J. M. Spraggins, *Ann. Rev. Anal. Chem.* **2024**, *17*, 1. c) K. K. Krestensen, R. M. A. Heeren, B. Balluff, *Analyst* **2023**, *148*, 6161. d) M. Planque, S. Igelmann, A. M. F. Campos, S. M. Fendt, *Curr. Opin. Chem. Biol.* **2023**, *76*, 102362. e) X. Ma, F. M. Fernandez, *Mass Spectrom. Rev.* **2024**, *43*, 235. f) C. T. McDowell, X. Lu, A. S. Mehta, P. M. Angel, R. R. Drake, *Mass Spectrom. Rev.* **2023**, *42*, 674.
[2] J. Franck, M. E. Ayed, M. Wisztorski, M. Salzet, I. Fournier, *Anal. Chem.* **2009**, *81*, 8305.
[3] a) M. Merdas, M. Lagarrigue, Q. Vanbellingen, T. Umbdenstock, G. Da Violante, C. Pineau, *J. Mass Spectrom.* **2021**, *56*, e4731. b) C. Harkin, K. W. Smith, F. L. Cruickshank, C. L. Mackay, B. Flinders, R. M. A. Heeren, T. Moore, S. Brockbank, D. F. Cobice, *Mass Spectrom Rev* **2022**, *41*, 662. c) Q. Zhou, A. Fulop, C. Hopf, *Anal. Bioanal. Chem.* **2021**, *413*, 2599.
[4] L. Ye, H. M. Zhang, B. J. Zhou, W. Tang, J. L. Zhou, *J. Chromatogr. A.* **2023**, *1706*, 464236.
[5] X. Bian, N. Li, B. Tan, B. Sun, M. Q. Guo, G. Huang, L. Fu, W. L. W. Hsiao, L. Liu, J. L. Wu, *Anal. Chem.* **2018**, *90*, 11210.
[6] N. de Haan, S. Yang, J. Cipollo, M. Wuhrer, *Nat. Rev. Chem.* **2020**, *4*, 229.
[7] a) M. Shariatgorji, A. Nilsson, E. Fridjonsdottir, T. Vallianatou, P. Kallback, L. Katan, J. Savmarker, I. Mantas, X. Zhang, E. Bezard, P. Svenningsson, L. R. Odell, P. E. Andren, *Nat. Methods* **2019**, *16*, 1021. b) P. Mielczarek, T. Slowik, J. H. Kotlinska, P. Suder, A. Bodzon-Kulakowska, *Molecules* **2021**, *26*, 2737.
[8] H. Zhang, X. Shi, N. Q. Vu, G. Li, Z. Li, Y. Shi, M. Li, B. Wang, N. V. Welham, M. S. Patankar, P. Weisman, L. Li, *Anal. Chem.* **2020**, *92*, 13361.
[9] S. Holst, B. Heijs, N. de Haan, R. J. van Zeijl, I. H. B.-D. Bruijn, G. W. van Pelt, A. S. Mehta, P. M. Angel, W. E. Mesker, R. A. Tollenaar, R. R. Drake, J. V. Bovee, L. A. McDonnell, M. Wuhrer, *Anal. Chem.* **2016**, *88*, 5904.
[10] a) T. T. Forsman, M. E. Duenas, Y. J. Lee, J. M. Spectrom **2021**, *56*, e4709. b) F. Waldchen, B. Spengler, S. Heiles, *J. Am. Chem. Soc.* **2019**, *141*, 11816. c) K. J. Zemaitis, V. S. Lin, A. H. Ahkami, T. E. Winkler, C. R. Anderton, D. Velickovic, *Anal. Chem.* **2023**, *95*, 12701. d) A. Bednarik, S. Bolsker, J. Soltwisch, K. Dreisewerd, *Angew. Chem. Int. Ed., Engl.* **2018**, *57*, 12092.
[11] R. Ju, X. Liu, F. Zheng, X. Zhao, X. Lu, Z. Zeng, X. Lin, G. Xu, *Anal. Chim. Acta* **2019**, *1067*, 79.
[12] B. Balluff, C. Hopf, T. P. Siegel, H. I. Grabsch, R. M. A. Heeren, *J. Am. Soc. Mass Spectrom.* **2021**, *32*, 628.
[13] V. L. Li, Y. He, K. Contrepois, H. Liu, J. T. Kim, A. L. Wiggenhorn, J. T. Tanzo, A. S. Tung, X. Lyu, P. H. Zushin, R. S. Jansen, B. Michael, K. Y. Loh, A. C. Yang, C. S. Carl, C. T. Voldstedlund, W. Wei, S. M. Terrell, B. C. Moeller, R. M. Arthur, G. A. Wallis, K. van de Wetering, A. Stahl, B. Kiens, E. A. Richter, S. M. Banik, M. P. Snyder, Y. Xu, J. Z. Long, *Nature* **2022**, *606*, 785.
[14] a) S. Xiao, V. L. Li, X. Lyu, X. Chen, W. Wei, F. Abbasi, J. W. Knowles, A. S. Tung, S. Deng, G. Tiwari, X. Shi, S. Zheng, L. Farrell, Z. Z. Chen, K. D. Taylor, X. Guo, M. O. Goodarzi, A. C. Wood, Y. I. Chen, L. A. Lange, S. S. Rich, J. I. Rotter, C. B. Clish, U. A. Tahir, R. E. Gerszten, M. D. Benson, J. Z. Long, *Nat. Metab.* **2024**, *6*, 659. b) B. Scott, E. A. Day, K. L. O'Brien, J. Scanlan, G. Cromwell, A. N. Scannail, M. E. McDonnell, D. K. Finlay, L. Lynch, *Nat. Metab.* **2024**, *6*, 651. c) S. Xiao, V. L. Li, X. Lyu, X. Chen, W. Wei, F. Abbasi, J. W. Knowles, S. Deng, G. Tiwari, X. Shi, S. Zheng, L. Farrell, Z. Z. Chen, K. D. Taylor, X. Guo, M. O. Goodarzi, A. C. Wood, Y. D. I. Chen, L. A. Lange, S. S. Rich, J. I. Rotter, C. B. Clish, U. A. Tahir, R. E. Gerszten, M. D. Benson, J. Z. Long, *BioRxiv* **2023**, *11*, 565321.
[15] A. M. J. van Wegberg, J. C. van der Weerd, U. F. H. Engelke, K. L. M. Coene, R. Jahja, S. J. L. Bakker, S. C. J. Huijbregts, R. A. Wevers, M. R. Heiner-Fokkema, F. J. van Spronsen, *J. Inherited Metab. Dis.* **2024**, *47*, 624.
[16] R. S. Jansen, R. Addie, R. Merkx, A. Fish, S. Mahakena, O. B. Bleijerveld, M. Altelaar, L. I. J., R. J. Wanders, P. Borst, K. van de Wetering, *Proc. Natl. Acad. Sci.* **2015**, *112*, 6601.
[17] A. Alexandridou, D. A. Volmer, *J. Lipid Res.* **2023**, *64*, 100409.
[18] T. Mukaiyama, *Angew. Chem.* **1976**, *89*, 858.
[19] a) P. Apostolova, E. L. Pearce, *Trends Immunol.* **2022**, *43*, 969. b) X. Li, Y. Yang, B. Zhang, X. Lin, X. Fu, Y. An, Y. Zou, J. X. Wang, Z. Wang, T. Yu, *Signal Transduct. Target Ther.* **2022**, *7*, 305.
[20] S. Broer, A. Broer, *Biochem. J.* **2017**, *474*, 1935.
[21] S. Crosignani, J. Gonzalez, D. Swinnen, *Org. Lett.* **2004**, *6*, 4579.
[22] R. Shariatgorji, A. Nilsson, E. Fridjonsdottir, N. Strittmatter, A. Dannhorn, P. Svenningsson, R. J. A. Goodwin, L. R. Odell, P. E. Andren, *Nat. Protoc.* **2021**, *16*, 3298.

Manuscript received: July 25, 2025
Revised manuscript received: August 23, 2025
Version of record online: September 8, 2025